Heterogenized molecular (pre)catalysts for water oxidation and oxygen reduction

Ham, C.J.M. van der

Author: Ham, C.J.M. van der
Title: Heterogenized molecular (pre)catalysts for water oxidation and oxygen reduction
Issue Date: 2019-10-10

5 | Phenanthroline immobilized on Au electrodes as ligand in copper-mediated oxygen reduction

Abstract

Upon the electrochemical reduction of an *in situ* generated 5-diazo-1,10-phenanthroline ion (**1**-NH_2^+), **1** can be covalently attached to a gold electrode. The grafted molecules act as ligand when brought in contact with a copper-containing electrolyte solution. As the ligands are limited in spatial movement, the formation of complexes with only one phenanthroline ligand is ensured. The *in situ* generated complexes are investigated in the oxygen reduction reaction. An overpotential of 800 mV is observed in the oxygen reduction reaction. During catalysis a thick copper layer is formed on the electrode surface, which covers the organic layer. Catalyst deactivation occurs due to a chemical transformation of the grafted layer and the partial disappearance of the organic layer.

"Earth is presently in a period of increasing heat released over time from many sources."
Patrick Dugan

In preparation for publication

5.1 Introduction

In the previous chapter, the oxygen reduction reaction was investigated with *in situ* generated copper phenanthroline complexes. Oxygen reduction with *in situ* generated copper complexes is only efficient with 1 to 1 ratio complex of copper to 1,10-phenanthroline was used, as higher ratios of 1,10-phenanthroline to copper yield little to no oxygen reduction activity.

Due to the low barrier for ligand exchange at copper, free copper is readily formed in solutions of copper ligated to one equivalent of phenanthroline. This results in deposition of a metallic copper layer on electrode surfaces under reductive potentials. As was shown in Chapter 3, also tridentate ligands can decoordinate under reductive conditions, forming a metallic copper layer on the electrode surface.

By immobilizing the 1,10-phenanthroline covalently to a gold electrode, the formation of a copper deposit on the gold surface is prevented, since gold surface is completely coated by the organic ligand (see Figure 5.1). In order to prevent the loss of copper from the surface adsorbed ligands, Cu^{II} is kept in the electrolyte solution during catalysis. This means that a large amount of copper which is present in the electrolyte solution is not catalytically active. The surface is no longer available for the deposition of copper and thus any catalytic activity observed should be from a molecular complex present at the electrode surface.

In the group of Chidsey, oxygen reduction was investigated using a copper complex with a 3-ethynyl-1,10-phenanthroline ligand immobilized covalently to an azide modified glassy carbon electrodes was investigated.[1] Oxygen reduction was determined to be second order in copper complex loading on the electrode surface. This means the triazole linker give the complexes on the electrode surface enough mobility to form a dinuclear complex on the electrode surface with oxygen bridging between the two copper centers. No copper was present in the electrolyte solution and the copper could be decoordinated by adding sodium diethyldithiocarbamate, a strongly copper chelating ion. No long term stability experiments were reported. One could imagine copper dissociating from the surface adsorbed ligand and leaching into the electrolyte, resulting in a loss of activity.

The formation of a surface adsorbed dimer should lead to second order kinetics in copper. By immobilizing the phenanthroline molecule to the electrode surface directly, thus without the triazole linker used by Chidsey *et al*, a rigid system is formed. The surface adsorbed complexes do not have the mobility to form dimers as the phenanthroline molecules are retained in a perpendicular fashion to the electrode surface.

The immobilization of organic molecules on electrode surfaces has been of interest over the last decades.[2–10] One possibility of immobilization is by forming a covalent bond which is formed by reducing a diazonium compound.[2, 4–6, 10] This diazonium cation can be formed *in situ* by the addition of sodium nitrite to an organic molecule containing an amine (Figure 5.2). The diazonium ion in turn is reduced in close proximity to the working electrode under reductive conditions and liberates nitrogen in the process. A radical remains on the position of the diazonium moiety. This radical can couple to the electrode, forming a covalent bond.

An advantage of the immobilization of **1** via the reduction of a diazonium ion is that it forms thin layers on the electrode.[5] Upon the reduction of 5-diazo-1,10-phenanthroline (**1**-N_2^+) at glassy carbon electrodes an organic layer with a thickness of 2 nm is formed.[6] Immobilization of **1** can also be performed by the reduction of 5-bromo-1,10-phenanthroline.[9] The thickness of the layer formed upon the reduction of 5-bromo-1,10-phenanthroline is 125 nm, which is much thicker than the layer formed by the reduction of **1**-N_2^+. Also the reduction of 1,10-phenanthroline itself leads to formation of an organic layer on the electrode. This direct reduction of 1,10-phenanthroline at glassy carbon electrodes happens at adsorbed 1,10-phenanthroline molecules via a proton coupled electron transfer step which leads to the formation of a carbon centered radical at the 4-position. The radical couples with the glassy carbon electrode, resulting in the loss of aromaticity on on one of the phenyl rings. The thickness of the organic layer on the electrode is approximately 2 nm thick, similar to the layer formed by the reduction of **1**-N_2^+.[6] Upon direct reduction of 1,10-phenanthroline,the molecules are in this case more upright than in the case of **1**-N_2^+. We anticipate that the geometry of the molecules at the electrode surface is more advantageous in the case of reduction of **1**-N_2^+ than of 1,10-phenanthroline.

The proposed mechanism of the reduction of diazonium ions does include the formation of a radical. Such radicals are highly reactive and consequently react with other radicals, forming diamagnetic dimers which do not attach to the electrode surface. It is also possible that the radicals react with molecules which are already attached to the electrode surface, forming thick layers of organic material on the electrode surface. This has been observed in the immobilization of 1,10-phenanthroline on glassy carbon electrodes.[6] Analysis of AFM studies of the grafted layer points to a layer thickness of 2 nm, which is more than twice the length of a phenanthroline molecule in the gas phase. The generated radicals may also react with residual oxygen. In summary, these side reactions mean the efficiency of the immobilization reaction can be rather low.

In this work, we present the covalent immobilization of 1,10-phenanthroline attached to gold surface by reduction of *in situ* generated 1,10-phenanthroline-5-diazonium ion. The immobilized phenanthroline moiety functions as a ligand for copper, which in turn is studied for the oxygen reduction reaction.

Copper ions are kept in solution during oxygen reduction in order to ensure the presence of copper near the electrode surface. These conditions were chosen because due to the fast ligand exchange kinetics copper will leach into the electrolyte if it is not present in the electrolyte solution. The catalytic experiments were performed in Cl^- containing electrolyte and acidified to ph 4, since Cu^{2+} does not dissolve in perchlorate containing electrolyte solutions.

5.2 Experimental

5.2.1 Reagents and materials

1,10-phenanthroline-5-amine (Sigma Aldrich, 97%), 4-bromoaniline (Sigma Aldrich, 99%), $NaNO_2$ (Merck, 99.9%), $K_3Fe(CN)_6$ (Sigma Aldrich, 99.98%) and $Cu(OTf)_2$ (Alfa Aesar, $\geq$ 99%) were used as received.

Electrolyte solutions were prepared with $HClO_4$ (Merck suprapur, 70 %), HCl (Merck, 37 %), Na_2HPO_4 (Merck, 99.9%), NaH_2PO_4 (Merck, 99.9 %), NaCl (Merck, 99.9 %) and were prepared with MilliQ water ($>$ 18.2 MΩ cm resistivity).

Argon and dioxygen (5.0) were purchased from Linde Gas.

5.2.2 Electrochemical methods

All electrochemical experiments were performed on an Autolab PGSTAT 128N with integrated EQCM module in one-compartment 25 ml glass cells in three-electrode setups. A gold working electrode (99.995 %, Alfa Aesar, 0.05 cm^2 geometric surface area) was used in a hanging meniscus configuration. Platinum (99.99%, Alfa Aesar) was used as a counter electrode and a Ag/AgCl (3

M KCl) purchased from Autolab was used as reference electrode.

The Au electrode was cleaned by oxidation at 10 V *versus* a graphite rod counter electrode in 10% H_2SO_4 for 30 s. This was followed by a 6 M HCl bath for 20 s, followed by flame annealing. The electrode was then electrochemically polished by cycling between 0 and 1.75 V *versus* RHE (E_{start} = 0.7 V) at 1 V s^{-1} in 0.1 M $HClO_4$.

Modification of gold electrodes was performed in 0.5 M HCl electrolyte with 1 mM 1,10-phenanthroline-5-amine (97%, Sigma Aldrich) or 4-bromoaniline (99 %, Sigma Aldrich). The solution was deaerated for 30 min with argon (Linde 5.0). After deaeration, 3.4 mg $NaNO_2$ (puriss, Sigma Aldrich) was added to the electrolyte solution. After 60 seconds, argon was blanketed over the electrolyte solution and a cyclic voltammogram was started. For the 4-bromoaniline, the Au electrode was cycled between -0.5 and 0.5 V *versus* Ag/AgCl at 100 mV s^{-1} for 5 cycles. For 1,10-phenanthroline-5-amine, the Au was cycled -0.2 and 0.3 V *versus* Ag/AgCl at 50 mV s^{-1} for 10 cycles.

Oxygen reduction experiments were performed in 0.05 M NaH_2PO_4 (99.99 %, Merck), 0.05 M Na_2HPO_4 (99.99 %, Merck), 0.05 M NaCl (99.99 %, Merck) and 0.6 mM HCl (37 %, VWR International). In case of catalytic experiments, 1 mM $Cu(OTf)_2$ was added to the electrolyte solution. Prior to oxygen reduction experiments, oxygen was bubbled through the electrolyte for at least 20 minutes, while during experiment, oxygen was blown over the solution.

Apart from the EQCM experiments and the experiments wherein the XPS samples are created, all electrochemical experiments were performed in a hanging meniscus configuration. In a hanging meniscus configuration, the electrode is situated in the headspace-electrolyte interface (left panel Figure 5.3). Prior to experiment, the electrode is not in contact with the electrolyte solution. The electrolyte containing 1 mM 1,10-phenanthroline-5-amine or 4-bromoanaline is deaerated using argon. After deaeration sodium nitrite is added as a solid to the electrolyte. One minute after addition of sodium nitrite, argon is blown over the headspace and the working electrode is brought in contact with the electrolyte, making a hanging meniscus. The area of contact between different experiments can differ slightly due to differences in the meniscus that is made.

5.2.3 EQCM setup

The electrochemical quartz crystal microbalance consisted of a PEEK cell purchased from Autolab. The cell was degassed with Ar (Linde, 5.0) prior to experiment. A gold working electrode (0.35 cm^2 geometric surface area) on a quartz crystal was used as received. Platinum was used as counter electrode and the experiments were measured *versus* a Ag/AgCl (3M KCl)reference electrode.

In the EQCM setup, the electrode is situated in the bottom of the cell (see right panel of Figure 5.3). This contrasts the electrochemical experiments wherein a hanging meniscus configuration was used, where the electrode sits in the liquid-headspace interface. The electrolyte-electrode interface cannot be broken during deaeration, thus in the EQCM setup the electrode is in contact with the electrolyte during deaeration. During this time, no potential is applied to the working electrode. Upon addition of sodium nitrite, the counter and reference electrodes are inserted into the electrolyte and the standby potential is applied. After one minute, cyclic voltammetry is started.

Since the EQCM oscillator needs to be warmed up prior to experiments, the cell was filled with 3 ml MilliQ water and the oscillator was turned on for 30 minutes. Simultaneously, the electrolyte solutions were prepared as described above. In quick succession, the following steps were taken: the $NaNO_2$ was added to the electrolyte solution; the EQCM oscillator was turned off; the MilliQ water in the EQCM cell replaced with the electrolyte solution and the oscillator was turned on. The modification was then started as described above.

5.3 Results and discussion

5.3.1 The reduction of diazonium ions for the covalent coupling of organic molecules to electrode surfaces

Since the reduction of diazonium compounds are highly dependent on the size of the electrode, a well-documented example from literature was reproduced. By reduction of *in situ* generated 4-bromobenzene-diazonium (**2**-N_2^+), **2** can be immobilized on the surface of the electrode. **2** is not expected to coordinate copper, when $Cu(OTf)_2$ is dissolved in the electrolyte. Moreover, the grafted layer formed on the electrode surface is not able to transfer electrons from the electrode to any redox-active species in the electrolyte solution. Therefore, copper from the electrolyte solution is not expected to form an active oxygen reduction catalyst.

Figure 5.4 illustrates the formation of **2** attached to gold (Au|**2**) via *in situ* reduction of 4-bromobenzene-diazonium (**2**-N_2^+). 5-diazo-1,10-phenanthroline(**1**-N_2^+) is generated *in situ* and reductively coupled to gold electrodes (Au|**1**, bottom panel in Figure 5.4). In contrast, **1** will be able to coordinate to copper and thus form a molecular oxygen reduction catalyst at the surface of the working electrode.

5.3.2 Coupling of 2 to gold electrodes by reduction of *in situ* generated 4-bromobenzene-diazonium

Several aryldiazonium compounds have been used to immobilize benzylic molecules at gold [2, 10] and glassy carbon electrodes.[4, 5, 10] In the group of Bèlanger, it was discovered a glassy carbon electrode grafted with **2** contains 0.38 nmol cm^{-2} using XPS.[4] In the cyclic voltammogram of reduction of **2** at glassy carbon, two peaks are observed. The first reduction peak is observed at 0.71 V *versus* RHE.[10] The nature of this peak is at present not fully understood. By scanning the potential up to this peak, partial blocking of the surface is observed in $K_3[Fe(CN)_6]$ blocking experiments. This peak is thus already associated with the reduction of **2**-N_2^+, but does not form a fully covered surface. The second reduction is associated with the reductive coupling of **2**-N_2^+ and **2**$^\bullet$ to the electrode surface and is observed at -0.09 V *versus* RHE. The peak is followed by a plateau reaching the vertex potential at -0.79 V *versus* RHE, which is also associated with the reduction of **2**-N_2^+ and the **2** radical. In the second scan of the cyclic voltammogram, the reductive peak is no longer visible.

Gooding *et al.* immobilized **2** via the reduction of the *in situ* generated **2**-N_2^+ at gold electrodes.[10] In the first scan of the cyclic voltammogram at a gold electrode, a reduction peak was reported at 0.36 V *versus* RHE. The peak is followed by a plateau. In the backward scan, the current drops to 0 A quickly. The reductive peak and the plateau are associated with the reduction of **2**-N_2^+ at the gold electrode. In the second scan, the peak and plateau are no longer visible. The differences in the cyclic voltammetry between glassy carbon and gold electrodes indicate the coupling of organic molecules is dependent on the electrode material and consequently that it is impossible to directly compare the reduction of diazonium ions at different electrode materials.

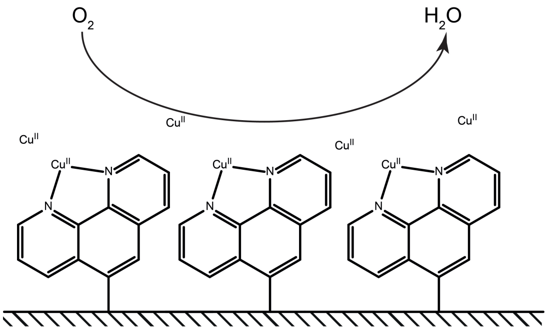

Figure 5.1: Schematic representations of inaccessibility of the gold surface due to the covalent attachment of organic molecules onto gold electrodes.

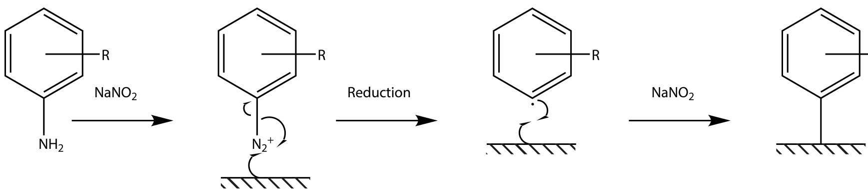

Figure 5.2: Generalized mechanism for the formation of a covalent bond between an electrode and an organic molecule by the reduction of an *in situ* generated diazonium ion.

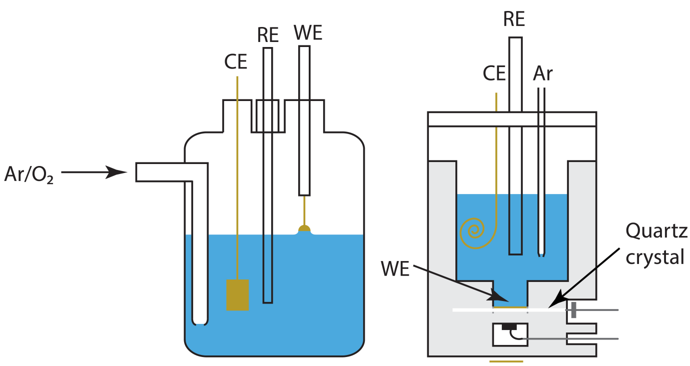

Figure 5.3: Schematic representations of electrochemical cells with an electrode used in hanging meniscus configuration (left) and the electrode sitting in the bottom of the EQCM cell (right)

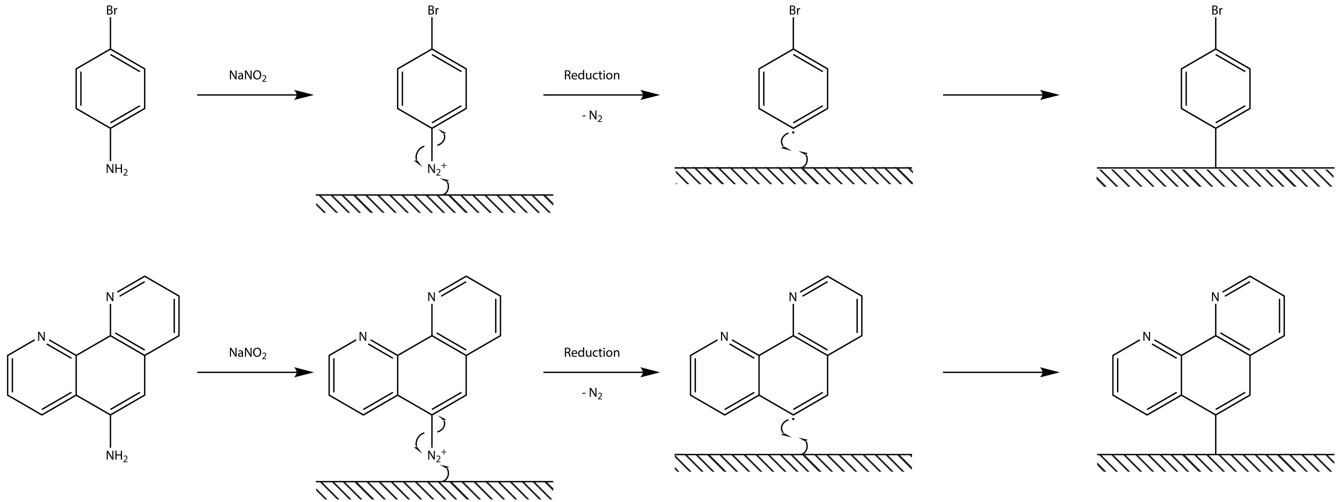

Figure 5.4: Proposed reaction mechanism of the immobilization of **2** (top) and **1** (bottom) onto a gold electrode by reduction of *in situ* generated diazonium ions.

In this study, the reductive coupling of **2** with the gold electrode was performed in a hanging meniscus configuration. In the first scan of the immobilization of **2**, a sharp reductive peak is observed at 0.34 V *versus* RHE. In the backward scan the current rapidly decreases to 0 A. The consecutive scan shows no reductive currents anymore, which indicates that the surface is fully covered with **2** after a single scan while scanning at 100 mV s^{-1}. No oxidation processes are observed between 0.71 and -0.29 V *versus* RHE in all the scans, indicating that no oxidative degradation of the organic layer takes place. The results reported here are in good agreement with the electrochemistry of **2**-NH_2 reported by Gooding *et al*. The formation of Au|**2** was further investigated using EQCM.

There is a difference in the surface area between the EQCM electrode (0.39 cm^2 real surface area) and the hanging meniscus electrode (0.05 cm^2 real surface area). Therefore differences in immobilization kinetics are expected due to different diffusion patterns. The real surface area of the working electrodes was determined *ex situ* by measuring the charge transferred during the reduction of the gold oxide formed in 0.1 M $HClO_4$ electrolyte solution.[11]

Using EQCM, the amount of **2** grafted onto the electrode surface was quantified. The reduction of the diazonium ion starts at 0.41 V *versus* RHE, as it did on the gold electrode in hanging meniscus configuration described above. A slow reduction process is observed over the whole forward scan below 0.41 V. The shape of the slow reduction of **2**-N_2^+ shown in the cyclic voltammogram is different from the cyclic voltammogram in hanging meniscus configuration due to the differences in diffusion behavior (see Figures 5.5 and 5.6). The total mass increase over the first scan is 145 ng cm^{-2}, as is shown in the top panel of Figure 5.6, which corresponds to approximately 0.9 nmol cm^{-2}.

The unit cell of a gold FCC latice has a lattice constant of 406.5 pm.[12] Since the diagonal of one of the faces contains 2 whole atomic diameters, one can calculate the atomic radius in the FCC lattice using Equation 5.1, where a is the lattice constant and r is the radius of a gold atom in the lattice.

$$(4\mathrm{r})^2 = 2\mathrm{a}^2 \text{ or } \mathrm{r} = \frac{1}{2\sqrt{2}}\mathrm{a} \text{ or } \mathrm{r} = \frac{1}{2\sqrt{2}} \times 406.5 = 143\,\mathrm{pm} \tag{5.1}$$

One gold atom in the (111) latices takes up 7.16×10^{-16} cm^2. The total surface of the EQCM electrode thus contains approximately 5.45×10^{14} atoms. This indicates a coverage of

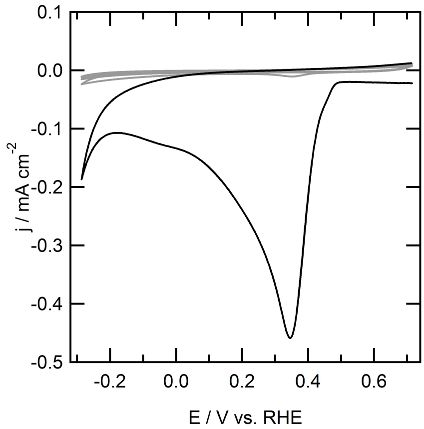

Figure 5.5: First scan (solid line) and second scan (dotted line) of electrochemical immobilization of **2** at a gold electrode (1.5 cm^2) in combination with EQCM of bromobenzene by reduction of a 1 mM **2**-N_2^+ ion solution generated *in situ* by addition of 4-bromoaniline and sodium nitrite to form a 1 mM solution of both in 0.5 M HCl electrolyte solution at 100 mV s^{-1}.

approximately 40 molecules of **2** per 100 gold atoms.

The total deposition of **2** measured by EQCM at a gold electrode (0.9 nmol cm^{-2}) is higher than the coverage found in the group of Bèlanger on glassy carbon electrodes measured *ex situ* by XPS spectroscopy (0.38 nmol cm^{-2}).[4]

During the reduction of the diazonium salts, carbon centered radicals are formed as intermediates (see Figure 5.2). These radicals are highly reactive, can dimerize or react with other species in solution, which results in a low faradaic efficiency. During the first cycle of the cyclic voltammogram, 371 μC cm^{-2} reductive current has been recorded. This means the faradaic efficiency of the formation of a Au-**2** bond by reduction of **2**-N_2^+ is approximately 48%.

In an outer sphere electron transfer process, there is no interaction between the electrode and a dissolved redox species. The electron transfer happens via tunneling through the electrolyte. An adsorbed layer on the electrode surface can block the tunneling of the electrons to the electrode if the layer adsorbed is thick enough and is not conducting. This allows us to investigate the conductivity of the grafted layers using a redox probe in solution. The conductivity

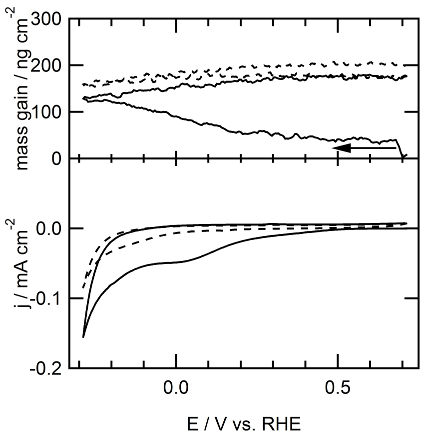

Figure 5.6: First scan (solid line) and second scan (dotted line) of electrochemical immobilization of **2** at a gold electrode (1.5 cm^2) in combination with EQCM of bromobenzene by reduction of a 1 mM **2**-N_2^+ ion solution generated *in situ* by addition of 4-bromoaniline and sodium nitrite to form a 1 mM solution of both in 0.5 M HCl electrolyte solution at 100 mV s^{-1}.

is of importance since during oxygen reduction, electrons need to transfer from the electrode to dissolved copper in the electrolyte in the blank. If no electron transfer is possible, no oxygen reduction activity is expected from dissolved copper species. When electron transfer through a grafted layer is observed, oxygen reduction could be a possibility. This should help predict the oxygen reduction behavior of the different grafted layers. For these experiments, $K_3[Fe(CN)_6]$ was used as it is known to react via outer sphere electron transfer processes.[10]

Gooding *et al.* attribute a redox couple with $E_{1/2} = 0.22$ V *versus* Ag/AgCl at a glassy carbon electrode to $K_3[Fe(CN)_6]$ via outer sphere electron transfer.[10] In the reduction of *in situ* generated **2**-N_2^+ on glassy carbon electrodes, two reduction events were observed, a first reduction peak at 0.71 V and a second reduction peak at -0.09 V *versus* RHE. By grafting the electrode over both reduction peaks, no redox chemistry of $K_3[Fe(CN)_6]$ was observed, indicating a total blockage of electron transfer to and from the glassy carbon electrode. Since no redox activity with $K_3[Fe(CN)_6]$ was observed the grafted layer must be thick enough to prevent fast tunneling through the layer. By scanning the electrode up to only the first reduction at 0.71 V, the na-

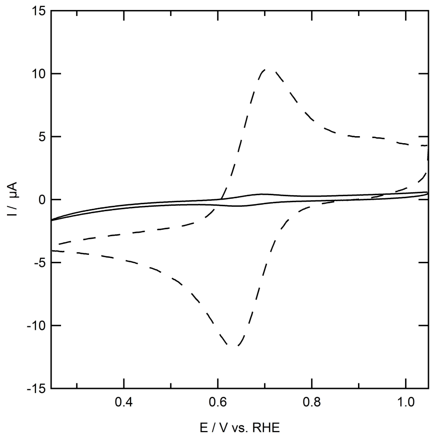

Figure 5.7: Outer sphere electron transfer at a gold electrode (dotted line) and a gold electrode modified with **2** using 1 mM $K_3[Fe(CN)_6]$ in 0.1 M phosphate buffer and 0.05 M NaCl at pH 7.

ture of the first reduction peak could be investigated. The peak current of the redox couple of $K_3[Fe(CN)_6]$ was halved, indicating the surface was partially blocked by **2**. This indicates grafting already starts at 0.71 V at a glassy carbon electrode. Apparently, full coverage of the surface has not been reached yet under these conditions.

In an outer sphere electron transfer process, there is no interaction between the electrode and the molecule in solution. Therefore the halfway potential ($E_{1/2}$) of the redox couple should remain the same. If the electron transfer kinetics becomes slower due to the presence of a grafted layer, an increase in ΔE is expected together with a lower maximum current. On a polished gold electrode, a Fe^{II}/Fe^{III} redox couple is observed with $E_{1/2}$ = 0.65 V (Figure 5.7). The peak of the oxidative wave is positioned at 0.29 V and with a peak current of 9.2 µA and the reductive peak lies at 0.61 V with a peak current of -10µA. If the surface is grafted with **2**, the current decreases twenty-fold while the peak potentials of the Fe^{II}/Fe^{III} redox couple remain more or less at the same position, with $E_{p,o}$ = 0.63 V and $E_{p,r}$ = 0.28 V, resulting in $E_{1/2}$ = 0.66 V. Since no apparent change in ΔE was observed, electron transfer must still occur at relatively fast rates. It therefore appears the surface of the gold electrode grafted with **2** is locally not completely covered. Since the surface exposed to the electrolyte might differ slightly each time a hanging meniscus is made,

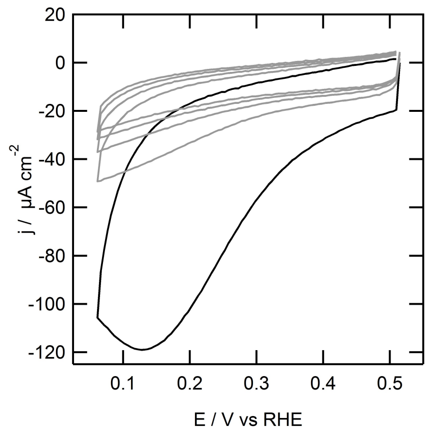

Figure 5.8: Immobilization of 1,10-phenanthroline on a gold electrode (0.05 cm^2) in hanging meniscus configuration from 1 mM **1**-N_2^+ ions formed*in situ* by addition of sodium nitrite and **1**-NH_2 to form a 1 mM solution of both to a 0.5 M HCl electrolyte solution at 50 mV s^{-1}.

the small redox couple observed after grafting is attributed to redox activity at parts of the gold electrode that was not exposed to the grafting electrolyte in the immobilization experiment.

5.3.3 Reductive coupling of *in situ* generated 5-diazo-1,10-phenanthroline to gold electrodes

The immobilization of **1** on glassy carbon electrodes was previously described by the group of Ekinci.[5] The immobilization was performed in 46% HBF_4 between -0.1 and -1.2 V *versus* Ag/AgCl (approximately 0.1 to -1.0 V *versus* RHE) at -4 ○C at 200 mV s^{-1}, while sodium nitrite was added dissolved in acetonitrile. Already at -0.1 V *versus* Ag/AgCl, a reductive current was observed. A double reduction peak was observed in the first scan, the first at -0.7 and the second at -0.9 V *versus* Ag/AgCl, which were attributed to the reduction of protonated 1,10-phenanthroline-5-amine and of the *in situ* generated diazonium ion. In the second and consecutive scans, the current decreased significantly, but the two reduction peaks remained visible. The surface coverage was determined to be 0.68 nmol cm^{-2} by XPS. The amount of **1** that is actually available for coordination was determined in the presence of [$RuCl_3$]. By hanging the grafted electrode in a [$RuCl_3$] solution and investigating the redox chemistry of the electrode afterwards, the number

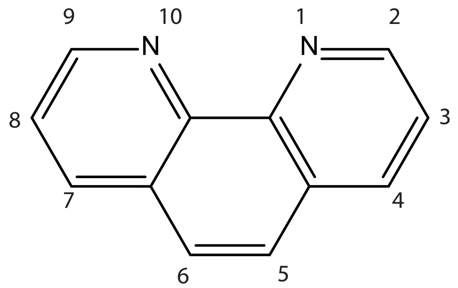

Figure 5.9: Numbering of substituents of 1,10-phenanthroline according to IUPAC convention.

of available sites on the surface was determined to be 0.36 nmol cm^{-2}.

Several other methods to immobilize phenanthroline onto gold electrodes have been reported as well.[6, 7, 9] In the group of Bertotti, 5-bromo-1,10-phenanthroline was reduced in DMF to form the radical on the 5- position on the phenanthroline ring either stepwise via 5-bromo-1,10-phenanthroline reduction to form a radical anion of 5-bromo-1,10-phenanthroline. Formation of this radical anion was followed by loss of Br^- leaving a radical at the position where the bromine left. At this position, phenanthroline, in turn could couple to the Au working electrode.[9] This forms a layer of Au|**1** on the electrode surface that in structure is identical to the reduction of the *in situ* generated **1**-NH_2. The thickness of the grafted layer was determined to be 125 nm using AFM. This indicates the formation of multiple layers of organic material on the surface of the electrode. Direct reductive coupling of 1,10-phenanthroline to glassy carbon was investigated in the group of Bèlanger.[6, 7] Reduction of 1,10-phenanthroline yields a coupling at the 4-position. On the other hand the reduction of *in situ* generated **1**-N_2^+ couples exclusively at the 5-position, since the radical formed on the phenanthroline molecule is situated in an sp-orbital and thus cannot migrate over the benzylic rings via its π-clouds. This implies that a different surface structure is obtained in case of **1**-N_2^+ reduction compared to reduction of 1,10-phenanthroline..

The reductive immobilization of **1** on gold was investigated using cyclic voltammetry in 0.5 M HCl solution (Figure 5.8). In contrast to the immobilization of **2**, the potential window was changed to 0.06 and 0.51 V, due to an oxidation observed above 0.51 V *versus* RHE. This oxidation is attributed to the formation of a ketone moiety on the 6-position.[3] At the start of the cyclic

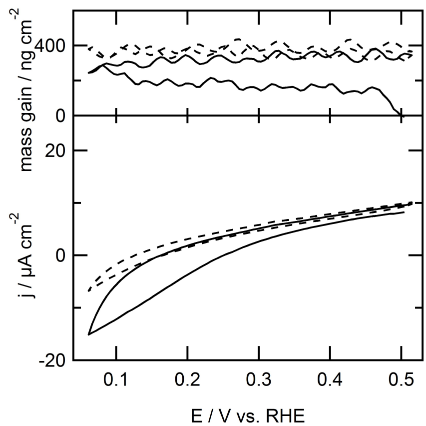

Figure 5.10: EQCM response of the first scan (solid line) and second scan (dotted line) of immobilization of **1** at a gold electrode (0.39 cm^2 geometric surface area) by reduction of a 1 mM **1**-N_2^+ ion solution generated *in situ* by addition of 1,10-phenanthroline-5-amine and sodium nitrite to form a 1 mM solution of both in 0.5 M HCl electrolyte solution at 50 mV s^{-1}.

voltammetry at 0.51 V, a reductive current is observed. The negative current increases as a more reducing potential is applied. At 0.11 V *versus* RHE, a peak is observed. In the backward scan, the current decreases rapidly. In each following scan, a decrease in current is observed at the vertex potential of 0.06 V. In the fifth and last scan, significant current can still be observed, suggesting **1**-N_2^+ is still being reduced in the fifth scan. Between different immobilization experiments of **1** under the same conditions, minor differences are observed with respect to the current and the peak position.

The amount of **1** that was immobilized on the gold electrode was quantified using EQCM (Figure 5.10). At the starting potential of 0.51 V an oxidative current of 8.2 μA is observed. It is unexpected that at the beginning of the experiment an oxidative current is observed. This current decreases linearly to 0 μA at 0.31 V *versus* RHE. Below 0.31 V, a reduction current is observed to continue to decrease until the vertex potential is reached. A weak shoulder can be observed between 0.21 and 0.11 V. In the backward scan, the current decreases to 0 A, after which a steady increase in oxidative current is observed increasing to 4 μA. Simultaneously with the cyclic voltammetry experiment, the mass of the electrode was measured using a microbalance. The mass of the electrode increases between 0.42 and 0.27 V *versus* RHE. This mass increase continues in the backward scan up till 0.42 V. In the second scan, the mass remains stable, indicating that no further modification of the electrode takes place. Most likely an outer sphere electron transfer that reduces **1** takes place, which results in dimerization of **1** in the electrolyte solution.

The reductive coupling of **1** at the EQCM electrode and the associated mass changes are displayed in Figure 5.10. At the start of the experiment at 0.5 V, an oxidative current is observed. Initially, the apparent mass of the electrode increases between the vertex potential of 0.51 V and 0.46 V. This increase in mass is most likely not associated with the reductive addition of of **1** to the electrode surface. After all, a positive current is still being measured under these conditions, which is at present not understood. We therefore do not take into account the initial mass increase between 0.51 and 0.46 V. The mass of the electrode increased by 77 ng cm^{-2} in the part of the voltammogram where reductive current is observed. This corresponds to 0.4 nmol cm^{-2} or 18 molecules of **1** per 100 gold atoms. A maximum of 50 molecules of **1** can be deposited on the surface of a gold (111) electrode, according to modeling experiments on Au|**1** (shown in Figure 5.11). The diameter of gold is 144 pm as was determined from the lattice constant.[12] The length of **1** was determined to be 6.6 nm by measuring the length of the molecule in ChemBioDraw 3D after energy minimization by MM2

$K_3[Fe(CN)_6]$ was used as a redox probe to investigate the surface blocking properties of **1** attached to the gold working electrode (Figure 5.12). Both redox peaks broaden with respect to the redox probe at a bare gold electrode, with $E_{p,o}$ = 0.78 V and $E_{p,r}$ = 0.51 V. The halfway potential $E_{1/2}$ is 0.65 V, which, as expected, is similar to the value found for the bare gold electrode. The peak current at the Au|**1** system drops to 5 μA, which is approximately half the peak current observed at the bare gold electrode. This drop in peak current and increased peak separation indicates that the outer sphere electron transfer rates from the electrode to the solution are retarded.

The current observed in the outer sphere redox behavior of **1** on gold differs from the immobilization of **1** on GC reported in the group of Ekinci.[5] They observed a large decrease in current and do not report discernible redox peaks of the $K_3[Fe(CN)_6]$ redox couple, but rather a positive and negative plateau. The higher surface blocking of the electrode observed by Ekinci

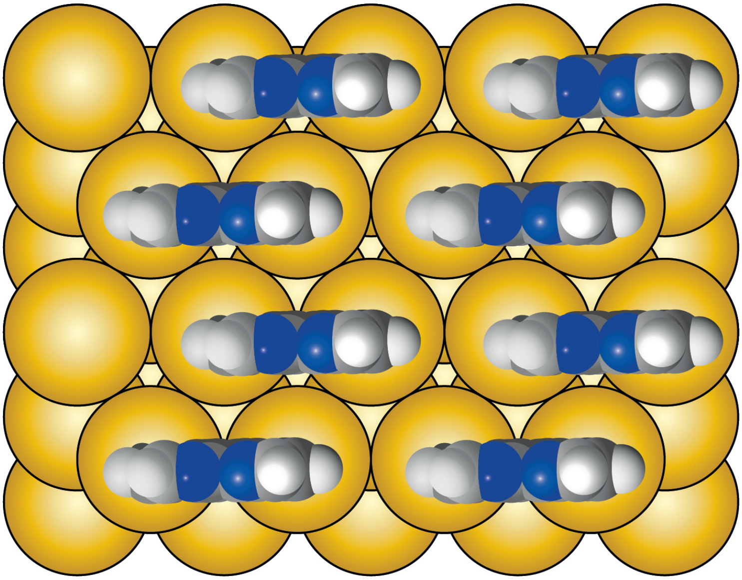

Figure 5.11: A gold (111) surface with the molecules of **1** for a well-ordered maximum surface coverage of 50 molecules of **1** per 100 Au surface atoms. The gold surface was made with the surface explorer[13] whereas the phenanthroline molecules were drawn in ChemBioDraw 3D. First an energy minimization was performed, after which the distance between the outer carbon atoms was measured. A gold diameter was 144 pm was selected.[12]

et al correlates well with the higher surface coverage that was observed in their experiments on glassy carbon.

5.3.4 Oxygen reduction activity of modified gold electrodes

In oxygen reduction experiments at immobilized catalysts it is important to rule out that any catalytic activity is due to uncovered electrode material. The activity of an unmodified gold electrode was therefore investigated between 0.63 and 0.23 V *versus* RHE in 0.1 M phosphate buffer and 0.05 M NaCl acidified to pH 4 using HCl. The onset potential for oxygen reduction is determined to be roughly 0.39 V, after which a catalytic wave is observed reaching -410 μA cm^{-2} at the lower vertex potential of 0.23 V.

Another important potential catalytic species that must be ruled out is deposition of copper

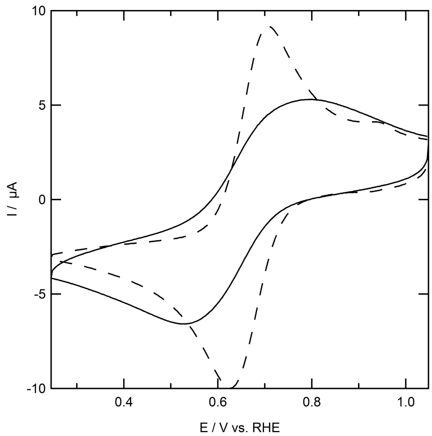

Figure 5.12: Outer sphere electron transfer at a gold electrode (dotted line) and a gold electrode modified with **1** using 1 mM $K_3[Fe(CN)_6]$ in 0.1 M phosphate buffer and 0.05 M NaCl at pH 7.

the gold electrode that forms under reductive potentials.[14, 15] Oxygen reduction at a gold electrode in presence of 1 mM Cu^{2+} was investigated using cyclic voltammetry between 0.25 and 0.75 V. In the cyclic voltammogram, a reductive current of -6 µA is observed at the vertex potential of 0.75 V *versus* RHE. Two reversible redox events are observed in the cyclic voltammogram of the Au|Cu^{II} system in presence of oxygen. The first redox couple has a reductive peak at 0.72 V and an oxidative peak above the vertex potential of 0.75 V. The second redox event has a reductive shoulder around 0.55 V, which underlies the other reductive peak and an oxidative peak at 0.72 V. These peaks are associated with copper deposition on the gold working electrode. Below 0.45 V, a catalytic wave is observed with a maximum current of -145 µA cm^{-2} at the vertex potential. It is surprising that oxygen reduction is suppressed by adding Cu^{2+} to the electrolyte solution. The current at 0.25 V in absence of Cu^{2+} is approximately three times higher than the current at a gold electrode in presence of Cu^{2+}.

At an electrode modified with **2** no outer sphere electron transfer with $K_3[Fe(CN)_6]$ is observed (see section 5.3.2). Since it is unlikely for **2** to bind copper ions from the solution. It is not expected that Au|**2**|Cu^{II} will show any oxygen reduction activity. The stability of such grafted layers is important to help understand the stability of Au|**1**. In the single sweep voltammetry of

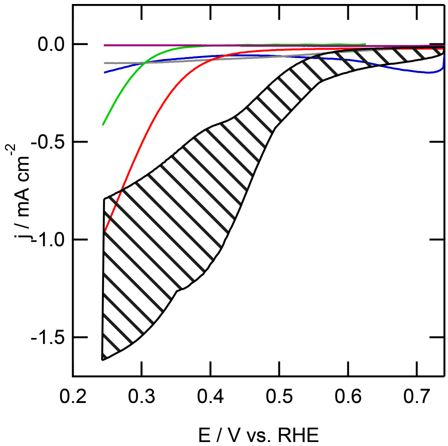

Figure 5.13: Electrochemical behavior of a bare gold electrode (green line), Au|**2**|Cu (purple), Au|Cu (blue line), Au|**1** (red line) and Au|**1**|Cu (black area) in presence of oxygen and Au|**1**|Cu in absence of copper (grey line) in 0.1 M phosphate buffer with 0.05 M NaCl acidified to pH 4 with HCl at 100 mV s^{-1}. The black area represents the spread of current observed over different oxygen reduction experiments.

Au|**2**|Cu^{II} in presence of oxygen, no current is observed. This shows that it is therefore possible to block oxygen reduction by grafting the electrode surface with a layer of organic molecules, even in the presence of dissolved copper species. Since no outer sphere electron transfer was observed with Au|**2**|Cu^{II}, two reasons for the absence of oxygen reduction could be given. First, there is the absence of electron transfer, meaning it is impossible to get electrons from the electrode to the surface via the grafted layer. Secondly, Au|**2** cannot coordinate to copper, indicating no surface immobilized complex can be formed to reduce oxygen.

In absence of copper, the electrode modified with **1** was investigated for the oxygen reduction reaction. Electron transfer is possible through the grafted layer as was observed in the surface blocking experiments using $K_3[Fe(CN)_6]$ (see section 5.3.3). Outer sphere reduction of O_2 therefore may still be possible and **1** immobilized on the gold electrode might act as an oxygen reduction catalyst as well. In the single sweep voltammogram, reductive current is observed with an onset potential of 0.45 V *versus* RHE. A catalytic wave with a maximum activity of 970 µA

cm^{-2} was observed. The current is 2.5 times higher than the oxygen reduction activity observed on an unmodified electrode in absence of copper (-970 μA cm^{-2} for Au|**1** *versus* -410 μA cm^{-2} for a bare gold electrode). With **1** immobilized on a gold electrode, the onset potential for the reductive current is shifted positively with 100 mV compared to an unmodified gold electrode in presence or absence of Cu^{II}.

An oxygen free solution of Au|**1**|Cu^{II} does not show any redox couples. Oxygen reduction at Au|**1**|Cu^{II} was observed with an onset potential that varied between 0.40 and 0.35 V *versus* RHE within different experiments. The activity at the lower vertex potential ranged between -0.80 to -1.6 mA cm^{-2} over different experiments. The onset shifted positively by 150 to 200 mV compared to the unmodified gold electrode in presence or absence of copper ions in solution, while the onset shifted 100 to 150 mV compared to Au|**1**. The activity is two to four times larger than the unmodified gold electrode in absence of Cu^{II} and equal to to two times larger than Au|**1**.

As mentioned above, the oxygen reduction activity for Au|**1**|Cu^{II} was not the same over all experiments. In some experiments a minor shoulder was observed between 0.50 and 0.30 V. The maximum current observed at the vertex potential of 0.25 V differed from -0.80 to -1.6 mA cm^{-2} in different experiments. The overpotential for oxygen reduction ranged from 0.83 to 0.88 V. In all experiments, the activity of the Au|**1**|Cu^{II} system surpassed the activity observed on a bare gold electrode. The differences in activity and onset potential could be due to the different surface structures formed by the reduction of **1**-N_2^+. With **1** attaching to **1** molecules which are already grafted onto the electrode surface, different surface structures can form during the reduction of **1**-N_2^+, which appears to be difficult to control. These differences could account for the differences observed in the catalytic activity of Au|**1**|Cu^{II} between different experiments. A different explanation could be the number of defects or the surface roughness, which could increase the number of **1** molecules adsorbed on the electrode surface.

In order to investigate the stability of the 1,10-phenanthroline immobilized system, cyclic voltammetry over 200 cycles was performed (Figure 5.14). A decrease in current is observed from 960 μA cm^{-2} in the first scan to 400 μA cm^{-2} in 200^{th} scan. Accompanied by the decrease in activity is the appearance of two oxidation and reduction peaks. There is an oxidation peak increasing with each scan at 0.55 V which is accompanied by a reduction at 0.47 V. The second redox couple has an oxidative peak at 0.73 and a reduction at 0.68 V.

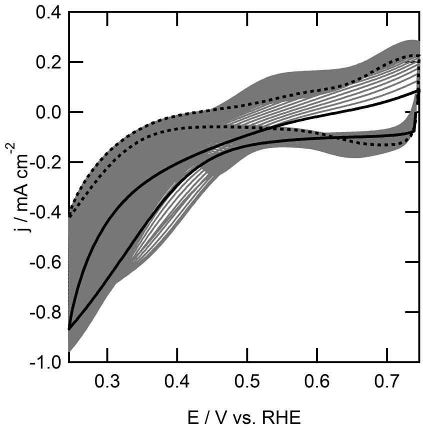

Figure 5.14: Electrochemical behavior of a gold electrode (0.05 cm^2 geometric surface area) grafted with **1** in presence of oxygen in 0.1 M phosphate buffer with 0.05 M NaCl acidified to pH 4 with HCl at 100 mV s^{-1}. First scan is depicted in black, 200th scan is depicted in dotted black line.

Apparently, the Au|**1**|Cu^{II} system is not a very stable system. The decrease in catalytic activity indicates that deactivation of the catalyst or degradation of the organic layer takes place. The Au-**1** bond could be broken and the complex may leach into the electrolyte solution. This would indicate that the gold surface becomes exposed to the electrolyte and that copper ions from the solution can adsorb onto the gold electrode. This would result in redox activity similar to the Au|Cu^{II} system. The redox couples do not completely match between Au|Cu^{II} and Au|**1**|Cu^{II} after 200 cycles of oxygen reduction. Another explanation could be the formation of thick copper layers on top of the phenanthroline layer. The composition of Au|**1**|Cu^{II} as a function of scan number and thus time was investigated by XPS.

5.3.5 XP spectra of Au|1 after different stages of oxygen reduction

The gold 4f peaks of the unmodified electrode are observed at 83.9 eV, which corresponds to literature values of 83.8 eV[16, 17] and 83.9 eV[18] (see Figure 5.15a). In the Au|**1** system, the binding energy and the total intensity of the Au 4f peak does not change, indicating that the adsorbed layer of **1** is very thin. After 25 cycles of oxygen reduction in the Au|**1**|Cu^{II} system a difference

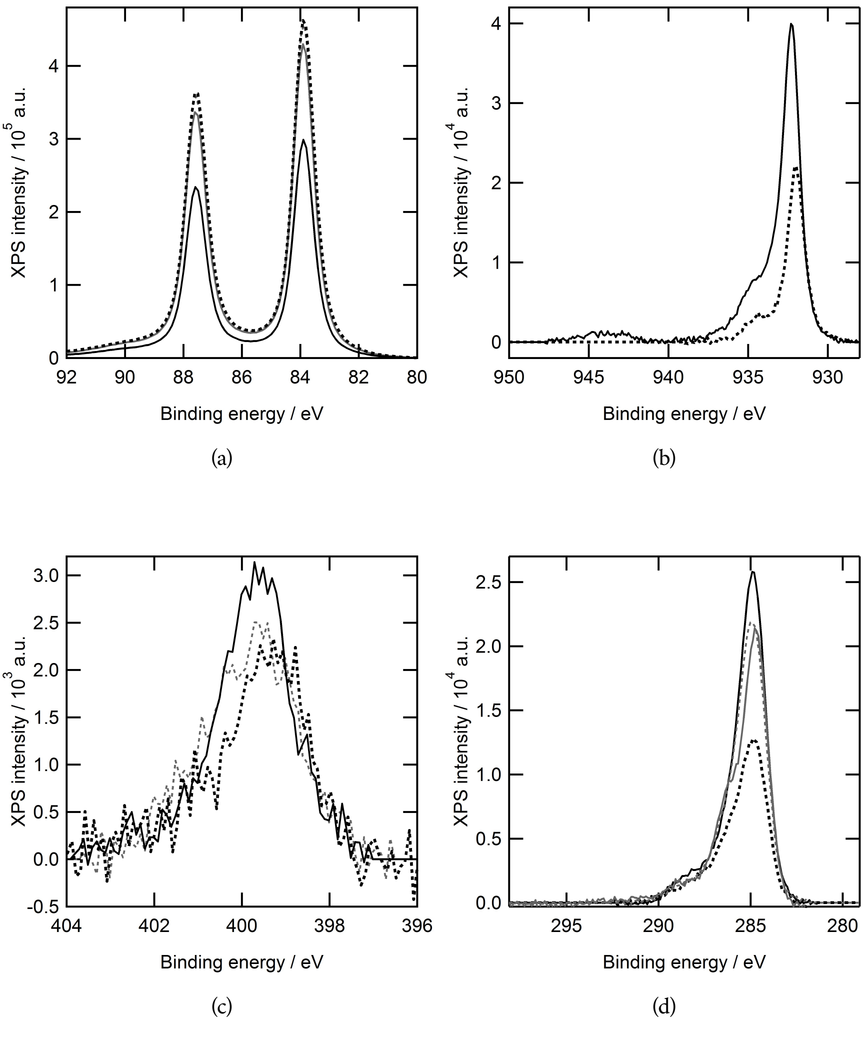

Figure 5.15: *Ex situ* X-ray photoelectron spectra of gold electrodes in the (a) Au 4f region, (b) Cu 2p region, (c) N 1s region and (d) C 1s region of an unmodified electrode (gray solid line), an electrode grafted with **1** (gray dotted line), after 25 cycles of oxygen reduction (black solid line) and after 200 cycles of oxygen reduction (black dotted line).

is observed, the intensity of the Au signals dropped by approximately 30%. 200 cycles of oxygen reduction brings the intensity of the gold 4f peaks back to the value of the unmodified electrode. The position of the peaks does not change during oxygen reduction or by immobilization of **1** on the electrode.

A copper layer is formed during oxygen reduction as is observed by the appearance of the Cu 2p peaks at 932.3 eV after 25 cycles of oxygen reduction (Figure 5.15b). This is in the same region where metallic copper and Cu(I) oxide is observed Literature reports values between 931.5 and 932.4 for Cu(0) and between 931.6 and 932.0 for Cu_2O.[19, 20] Weak satellites are observed between 940 and 947 eV, which is indicative of the presence of Cu(I) oxide.[21] When 200 cycles of oxygen reduction is performed, the total intensity of copper decreases to approximately 50% of the value observed after 25 cycles of oxygen reduction. The peak position shifts to a lower binding energy of 932.0 eV and the satellites between 490 and 497 eV disappear, indicating the copper present may be metallic Cu(0). The decrease in intensity for the Cu 2p peaks is reflected in the higher intensity for the Au 4f peaks, where the intensity returned to values similar to a bare gold or an electrode grafted with **1**.

The N 1s signals of the grafted electrode are observed at 399.6 eV (Figure 5.15c). Upon performing 25 cycles of oxygen reduction, the peak position and XPS intensity do not differ significantly compared to the electrode prior to the catalytic reaction. After 200 cycles of oxygen reduction the binding energy shifts to a slightly lower binding energy of 399.3 eV. This indicates a structural change of the organic layer which must still be present on the electrode surface, which could possibly be the formation of an N-oxide species.

The modified electrode changes during oxygen reduction catalysis. Initially, the electrode is grafted with a thin layer of **1** as the intensity of the gold 4f peaks does not change. After 25 cycles of oxygen reduction, a copper layer is present on the electrode surface, while an organic layer still appears to be present between the electrode and the copper layer. This is observed from a decrease in intensity of the Au 4f peaks, while the carbon and nitrogen peaks are still present in approximately the same intensity. Moreover the copper 2p peaks are present and show weak satellites, which indicates the adsorbed copper is in a reduced form. After 200 cycles of oxygen reduction, the amount of copper on the electrode is halved compared to 25 cycles of oxygen reduction. Also the carbon content is halved, indicating the layer of **1** is undergoing chemical changes. The intensity of the Au 4f peaks is at approximately the same level as a bare gold electrode. The degradation of the catalyst is also observed in the oxygen reduction activity. At the first 30 scans, the oxygen reduction activity increases, after which it keeps decreasing (Figure 5.14).

5.4 Conclusion

By immobilizing **1** at a gold electrode, oxygen reduction catalysis could be performed in an electrolyte solution containing Cu^{2+} At the start of the catalytic reaction the organic layer is still intact. During catalysis a layer of copper grows on the electrode surface which is accompanied by an increase in catalytic activity. During long term voltammetric cycling there is a change in the structure of the organic layer. As part of this structural change in the copper layer on the electrode surface is diminished while the oxygen reduction activity decreases.

Although the Au|**1**|Cu^{II} system forms an active oxygen reduction catalyst, it is not suitable for an application in an electrochemical cell, as the long-term stability is low and the overpotential is too high. However it is suitable for mechanistic studies, potentially making it a valuable tool in elucidating the mechanism of the oxygen reduction reaction.

5.5 References

(1) McCrory, C. C. L.; Devadoss, A.; Ottenwaelder, X.; Lowe, R. D.; Stack, T. D. P.; Chidsey, C. E. D. *J. Am. Chem. Soc.* **2011**, *133*, 3696–3699.

(2) Laforgue, A.; Addou, T.; Bélanger, D. *Langmuir* **2005**, *21*, 6855–6865.

(3) Gayathri, P.; Senthil Kumar, A. *Langmuir* **2014**, *30*, 10513–10521.

(4) Baranton, S.; Bélanger, D. *J. Phys. Chem. B* **2005**, *109*, 24401.

(5) Yeşildağ, A.; Ekinci, D. *Electrochim. Acta* **2010**, *55*, 7000–7009.

(6) Shul, G.; Weissmann, M.; Bélanger, D. *Electrochim. Acta* **2015**, *162*, 146–155.

(7) Shul, G.; Weissmann, M.; Bélanger, D. *Langmuir* **2014**, *30*, 6612–6621.

(8) Roy, F.; Et Taouil, A.; Lallemand, F.; Heintz, O.; Moutarlier, V.; Hihn, J.-Y. *Ultrason. Sonochem.* **2018**, *40*, 9–16.

(9) Valencia, D. P.; de Souza, A. P. R.; Gonçales, V. R.; Antonio, J. L. S.; Cordoba de Torresi, S. I.; Bertotti, M. *Electrochem. Commun.* **2014**, *38*, 32–35.

(10) Liu, G.; Chockalingham, M.; Khor, S. M.; Gui, A. L.; Gooding, J. J. *Electroanal.* **2010**, *22*, 918–926.

(11) Trasatti, S.; Petrii, O. A. *J. Electroanal. Chem.* **1992**, *327*, 353–376.

(12) Davey, W. P. *Phys. Rev.* **1925**, *25*, 753–761.

(13) Surface Explorer.

(14) Li, Q.; Xu, P.; Zhang, B.; Tsai, H.; Zheng, S.; Wu, G.; Wang, H.-L. *J. Phys. Chem. C* **2013**, *117*, 13872–13878.

(15) Awad, M. I.; Ohsaka, T. *Journal of Power Sources* **2013**, *226*, 306–312.

(16) Dückers, K.; Bonzel, H. P. *Surf. Sci.* **1989**, *213*, 25–48.

(17) Bird, R. J.; Swift, P. *J. Electron Spectros. Relat. Phenomena* **1980**, *21*, 227–240.

(18) Bravo, B. G.; Michelhaugh, S. L.; Soriaga, M. P.; Villegas, I.; Suggs, D. W.; Stickney, J. L. *J. Phys. Chem* **1991**, *95*, 5245–5249.

(19) Ertl, G.; Hierl, R.; Knözinger, H.; Thiele, N.; Urbach, H. *Appl. Surf. Sci.* **1980**, *5*, 49–64.

(20) Klein, J. C.; Proctor, A.; Hercules, D. M.; Black, J. F. *Anal. Chem.* **1983**, *55*, 2055–2059.

(21) Scrocco, M. *Chem. Phys. Lett.* **1979**, *63*, 52–56.